Effects of backflow correlation in the three-dimensional electron gas: Quantum Monte Carlo study

Yongkyung Kwon
Department of Physics and Center for Advanced Materials and Devices, Kon-Kuk University, Seoul 143-701, Korea

D. M. Ceperley
Department of Physics and National Computational Science Alliance, University of Illinois, Urbana, Illinois 61801

Richard M. Martin
Department of Physics and Materials Research Laboratory, University of Illinois, Urbana, Illinois 61801
(Received 16 January 1998)

The correlation energy of the homogeneous three-dimensional interacting electron gas is calculated using the variational and fixed-node diffusion Monte Carlo methods, with trial functions that include backflow and three-body correlations. In the high-density regime ($r_s \leqslant 5$) the effects of backflow dominate over those due to three-body correlations, but the relative importance of the latter increases as the density decreases. Since the backflow correlations vary the nodes of the trial function, this leads to improved energies in the fixed-node diffusion Monte Carlo calculations. The effects are comparable to those found for the two-dimensional electron gas, leading to much improved variational energies and fixed-node diffusion energies similar to the released-node energies of Ceperley and Alder. [S0163-1829(98)00135-0]

I. INTRODUCTION

The homogeneous electron gas in three dimensions is the simplest model to study the effects of correlation between electrons in metals.[1] Its correlation energy, defined as the total ground-state energy minus the Hartree-Fock energy, has been used to give the exchange-correlation potential in density-functional calculations with the local-density approximation.[2,3] The possible phases that this simple system can display are prototypes for understanding interacting electrons in extended matter.[4–8]

The theoretical study of the interacting electron gas began with Bloch[4] who discovered by using the Hartree-Fock approximation that the system would favor a ferromagnetic liquid state over the normal paramagnetic state at low electron densities. Wigner[5] first calculated the correlation energy of the homogeneous electrons at high-density limit, using the second-order perturbation theory. He also pointed out that for sufficiently low densities the electrons would become localized and form an ordered array. After calculating the correlation energy of this electron solid with the Wigner-Seitz approximation,[1,8] he proposed an interpolation formula for the correlation energy in a wide range of densities having his high- and low-density limits. The development of the field-theoretic approaches in the 1950s led to various approximate methods[8] to calculate the ground-state properties of the electron gas. Among them, Gell-Mann and Brueckner[9] summed the ring diagrams to compute the correlation energy in the high-density limit. The dielectric function formalism, especially with the self-consistent treatment of the screening process introduced by Singwi, Tosi, Land, and Sjölander,[10] gave more accurate ground-state properties at a wider range of densities.

On the other hand, various stochastic numerical methods, known collectively as quantum Monte Carlo (QMC) methods, have been developed to compute the properties of a quantum many-body system such as the electron gas. Ceperley[11] first applied variational Monte Carlo (VMC) methods to calculate a much more accurate upper bound to the ground-state energy of the electron gas than is given by Hartree-Fock methods. More accurate correlation energies were computed by Ceperley and Alder[12] with the diffusion Monte Carlo (DMC) method that projects the true ground state of a many-body system from a trial state. Even though the DMC method gives the exact ground-state energy for a system of many bosons, it has a serious difficulty in treating fermion systems, because fermion wave functions must be antisymmetric under particle exchanges.[13] In order to address this problem, Ceperley and Alder[12] developed the released-node method. Its only limitation is that the statistical fluctuations can grow rapidly at large projection time. So the statistical noise can dominate the signal before converging to the ground state.

In this paper, we use the fixed-node method,[14,12,15] where the nodal surface of the exact ground-state wave function is approximated by that of the trial wave function. We adopt the approach of systematically improving the fixed-node DMC results by using a trial function with better nodes, analogous to our work on the two-dimensional electron gas.[16] Unlike the released-node method this method is stable and does not have the convergence problem. It gives the best upper bound to the exact energy consistent with the assumed nodes.

Ceperley and Alder used the Slater-Jastrow trial wave function in both released-node[12] and fixed-node calculations,[17] which consists of the Slater determinant of single-body orbitals (plane waves for a homogeneous liquid phase) and products of two-body correlation functions. According to their released-node calculation, the electron gas could exhibit three different phases at zero temperature, the

 © 1998 The American Physical Society

paramagnetic and ferromagnetic liquids and the Wigner crystal, depending on its density. More recently, Ortiz and Ballone[18] reported a new fixed-node DMC calculation with the Slater-Jastrow wave function. Their correlation energies were found to be, as expected, smaller in magnitude than Ceperley and Alder's released-node calculations, especially at high metallic densities. In this paper, we report results of a fixed-node DMC calculation using a trial function with backflow and three-body correlations in addition to two-body correlation. Our previous calculations in the two-dimensional electron gas[16] showed that the inclusion of the backflow correlation in a trial state greatly improved the fixed-node result beyond that given by the Slater-Jastrow function. This is similar to what has been observed on calculations of the other strongly correlated system of fermions, liquid ^{3}He.[19] Our fixed-node DMC results in three dimensions will be compared with Ceperley and Alder's released-node results.

All ground-state properties of the electron gas at zero magnetic fields are determined only by the dimensionless density parameter $r_s = a/a_0$, where a_0 is the Bohr radius, $a = (3/4\pi\rho)^{1/3}$ is the radius of a sphere that encloses one electron on the average and ρ is the number density. With energy units of Rydbergs (Ry) and the length units of a, the Hamiltonian of the electron gas is

$$H = -\frac{1}{r_s^2}\sum_{i=1}^{N} \nabla_i^2 + \frac{2}{r_s}\sum_{i<j} \frac{1}{|\mathbf{r}_i - \mathbf{r}_j|} + \text{const}, \tag{1}$$

where the constant is the term due to the uniform background of opposite charge. We consider the density range of $1 \leqslant r_s \leqslant 20$, where Ceperley and Alder found the system in the normal liquid phase. We do not consider spin-polarized or superconducting states.

II. METHODOLOGY

In a VMC calculation, one estimates the properties of a quantum state, by assuming a trial wave function $\Psi_T(R)$ with the correct symmetry, where $R = (\mathbf{r}_1, \mathbf{r}_2, \ldots, \mathbf{r}_N)$ is a $3N$-dimensional vector representing the positions of N particles. With a set of configurations $\{R_i\}$ sampled with a probability density proportional to $\Psi_T^2(R)$, the variational energy is just the average of local energies, $E_L(R_i) = H\Psi_T(R_i)/\Psi_T(R_i)$. This method can give a good upper bound to the exact energy if the trial state is accurate as it is for the homogeneous electron gas.[11]

Even more accurate ground-state properties of a many-body system can be obtained with the DMC method, where the Schrödinger equation is solved by treating it as a diffusion equation.[12] The solution of the Schrödinger equation in imaginary time t, $-\partial|\Phi\rangle/\partial t = (\hat{H} - E_T)|\Phi\rangle$, can be expressed in terms of the exact energy eigenvalues E_i and eigenstates ϕ_i:

$$\Phi(R,t) = \sum_i c_i \exp[-t(E_i - E_T)]\phi_i(R). \tag{2}$$

At sufficiently long times only the ground state ϕ_0 survives in Eq. (2), if $\Phi(R,0)$ is not orthogonal to it. In order to implement this idea with a stochastic procedure, we consider the real-space representation of the Schrödinger equation:

$$\frac{\partial f(R,t)}{\partial t} = \frac{1}{r_s^2}\sum_{i=1}^{N} \nabla_i \cdot (\nabla_i f - f\nabla_i \ln\Psi_T^2) - [E_L(R) - E_T]f, \tag{3}$$

where $f(R,t) = \Phi(R,t)\Psi_T(R)$. Note that the Schrödinger equation is multiplied by the trial wave function $\Psi_T(R)$. Equation (3) can be viewed as a diffusion equation in a $3N$-dimensional space with the density of diffusing particles $f(R,t)$. Its second term imposes a drift and the final term gives rise to a branching process by which the sampled configurations converge to the lowest-energy state. The initial ensemble of configurations $\{R\}$ with probability density $f(R,0) = \Psi_T^2(R)$ is evolved forward in time by the above diffusion equation and reaches the equilibrium distribution $f(R,\infty) = \phi_0(R)\Psi_T(R)$ at large enough t. From this distribution of random walks, the exact ground-state energy $E_0 = \langle\phi_0|\hat{H}|\Psi_T\rangle/\langle\phi_0|\Psi_T\rangle$ can be estimated as the average of the local energy: $E_L(R) = H\Psi_T(R)/\Psi_T(R)$.

The diffusion equation formulation described above requires for implementation that the population density $f(R,t)$ be non-negative. For Bose systems, this is not a problem since their ground-state wave functions can be chosen to be non-negative. However, fermion wave functions are antisymmetric, change sign, and have nodes. This leads to the famous *sign problem*[13] in the QMC calculations of Fermi systems. The apparent limitation of the diffusion analogy in this case can be dealt with by treating positive and negative regions separately. One easy way to accomplish this is not to allow diffusion between these two regions, which corresponds to the *fixed-node* approximation.[14,12] If Ψ_T were to have the exact nodes of the ground state, one could treat the fermion system immediately and exactly, since f would never change sign. Unfortunately, the exact location of the nodes in many-fermion systems is not known.[20] The fixed-node approximation is based on the requirement that $\phi_0(R)\Psi_T(R)$ be non-negative. The fixed-node DMC energy is an upper bound to the exact energy, the best upper bound with the given nodes, and usually lies well below the variational energy.[20]

Another way to deal with the sign problem is to use the released-node method,[12] which puts no constraints on the nodal structure of the true ground-state wave function. In this method, there is a population of positive random walks that give positive contributions to any average, and a population of negative walks with negative contributions. Whenever a random walk diffuses across the nodes of the trial function, the sign of its contribution changes. Even though it can be shown that the population of the difference converges to the antisymmetric fermion ground state, it does not proceed without problems. Since both the positive and negative populations grow geometrically with long projection time t, the statistical fluctuations in the average increase exponentially.[12] For this method to be successful, the diffusion process needs to converge to the ground state before the fluctuations become large. Since the fluctuations grow as the system size gets larger, the released-node method becomes more difficult for systems with many fermions, and there is increased advantage in using the fixed-node method with nodes given by improved trial functions.

TABLE I. Optimized variational parameters of *three-body* and *backflow* correlation functions for $N=54$. δx is the average change in the nodal position due to the backflow correlation.

r_s	λ_B	s_B	r_B	w_B	λ_T	r_T	w_T	δx
1.0	0.025	0.395	0.210	0.689	0.006	0.293	0.949	0.0191(1)
5.0	0.105	0.158	0.180	0.670	-0.060	0.286	1.176	0.0580(1)
10.0	0.959	-0.672	0.247	3.788	-0.258	0.257	0.918	0.0657(1)
20.0	1.249	-0.938	0.275	3.787	-0.255	0.252	0.911	0.0549(1)

III. MONTE CARLO CALCULATIONS

A. Trial wave function

In all QMC methods mentioned above, a good trial function is very important for accurate results. The convergence time in a released-node calculation can be reduced with a better trial function while the nodes of a trial function determine the ultimate accuracy of a fixed-node calculation. The usual choice of a trial function is of the Slater-Jastrow type, which considers only two-body correlations [see Eq. (4) of Ref. 16]. The nodes of the wave function are determined by only the Slater determinant. We use the two-body correlation function that minimizes the variational energy in the random-phase approximation.[21] This trial wave function has been used in the previous VMC,[11,18] fixed-node DMC,[17,18] and released-node DMC calculations[12] to investigate the ground-state properties of the electron gas.

In order to improve the nodes, we consider a more complicated trial function,[16] which includes backflow and three-body correlations. Our wave function has the form

$$\Psi_T(R)=\det(e^{i\mathbf{k}_i\cdot\mathbf{x}_j})\exp\left[-\sum_{i<j}^{N}\tilde{u}(r_{ij})-\frac{\lambda_T}{2}\sum_{l=1}^{N}\mathbf{G}(l)\cdot\mathbf{G}(l)\right], \tag{4}$$

where $\mathbf{x}_i$'s are *quasiparticle* coordinates defined as

$$\mathbf{x}_i=\mathbf{r}_i+\sum_{j\neq i}^{N}\eta(r_{ij})(\mathbf{r}_i-\mathbf{r}_j). \tag{5}$$

The displacement of the quasiparticle coordinates $\mathbf{x}_i$ from the real coordinates $\mathbf{r}_i$ incorporates effects of hydrodynamic *backflow*,[22] and changes the nodes of the trial wave function. The backflow correlation function η is parametrized as

$$\eta(r)=\lambda_B\frac{1+s_Br}{r_B+w_Br+r^4}, \tag{6}$$

which has the long-range behavior ($\sim 1/r^3$) in three dimensions predicted by the local-energy method of Ref. 16 (though this behavior is smoothed by the periodic boundary conditions). Three-body correlation is included through the vector functions

$$\mathbf{G}(l)=\sum_{i\neq l}^{N}\xi(r_{li})(\mathbf{r}_l-\mathbf{r}_i). \tag{7}$$

We call $\xi(r)$ the three-body correlation function, for which we take the same functional form as in our previous study of the two-dimensional electron gas [see Eq. (15) of Ref. 16].

Our calculations are done for N electrons in a cube with the periodic boundary conditions. The Ewald method[23] is used for the Coulomb potential and the two-body correlation to minimize size effects. The higher-order correlation functions $\eta(r)$ and $\xi(r)$ are required to go to zero smoothly at a cutoff distance r_c, which is set to half the side of the simulation cell, as in Eq. (13) of Ref. 16.

In order to optimize our higher-order correlation functions, we minimize the variance of the local energy.[24] If our trial function Ψ_T were an exact eigenfunction of the Hamiltonian, the variance would be zero. Because the variance is a nonlinear function of the parameters we cannot be certain that we have achieved converged results for this class of trial functions. The optimum variational parameters that we have obtained as a function of density are given in Table I.

Figure 1 shows the three-body contribution to the logarithm of the wave function due to three electrons aligned and separated by a distance r. Note that this contribution has a strong density dependence. The effect is almost negligible at $r_s=1$ but as large as 7% at $r_s\geqslant 10$. Negative values imply that electron configurations in which the local environment is not ''balanced'' are slightly enhanced; for these configurations the true wave function is larger than the Slater-Jastrow pair product wave function.

Figure 2 shows the magnitude of the displacement of the quasiparticle coordinate caused by an electron a distance r away. The strongest effects are observed when two electrons are very close, for distances less than the average nearest-neighbor distance, which is 2 in the units we have used. We also note that a backflow potential has an attractive tail for $r_s\geqslant 10$. We calculated the average distance between the real and the quasiparticle coordinates during a VMC calculation with the backflow wave function. The average difference,

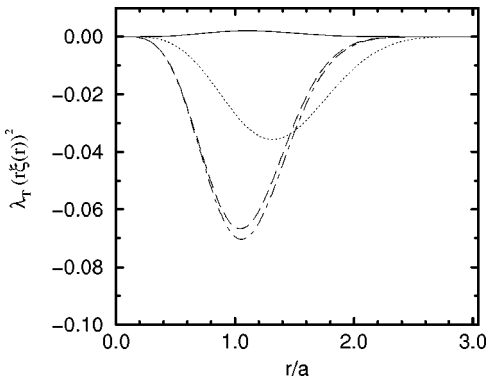

FIG. 1. The three-body contribution to the logarithm of the wave function due to three electrons aligned and separated by a distance r. Solid line, $r_s=1$; dotted line, $r_s=5$; dot-dashed line, $r_s=10$; long dashed line, $r_s=20$.

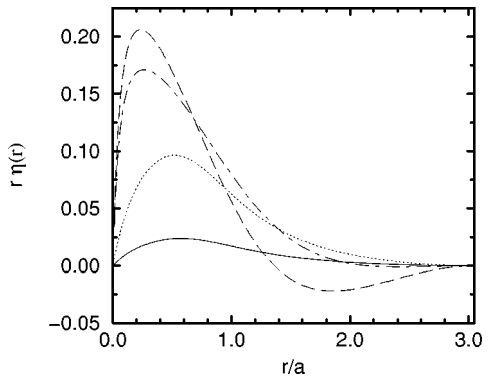

FIG. 2. The change in the quasiparticle coordinate caused by an electron a distance r away. Solid line, $r_s=1$; dotted line, $r_s=5$; dot-dashed line, $r_s=10$; long dashed line, $r_s=20$.

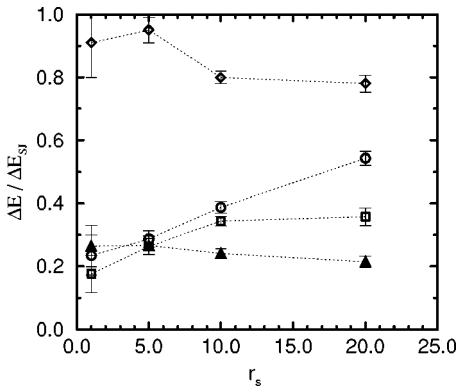

FIG. 3. Effects of *three-body* and *backflow* correlations as a function of the density of the system. The vertical axis shows $\Delta E/\Delta E_{SJ}=(E-E_{FN}^{3BF})/(E_{VMC}^{SJ}-E_{FN}^{3BF})$, that is, top axis corresponds to the Slater-Jastrow variational energy E_{VMC}^{SJ} and bottom axis to the fixed-node DMC energy E_{FN}^{3BF}, calculated with our best trial function including *three-body* and *backflow* correlations. The diamonds show the effect of only *three-body* correlation, the circles the effect of only *backflow*, and the squares represent the combined effect of both correlations. Finally, the filled triangles show the result using the fixed-node DMC method with free-fermion nodes of the Slater-Jastrow function.

defined as $\delta x=\langle|\mathbf{x}_i-\mathbf{r}_i|\rangle$, is shown in Table I. The displacement of the quasiparticle coordinate relative to the actual coordinate is about 1% of the interparticle spacing at $r_s\leqslant 1$ and 3% for $r_s\geqslant 5$. This implies that a released-node calculation with a relatively short projection time should be able to correct the nodal surfaces from those of a free fermion trial function.

The main difficulties in the use of the backflow wave function is that firstly, the implementation is considerably more complex than for the Slater-Jastrow form, and secondly, because update formulas cannot be used to speed up single particle moves, Monte Carlo moves are updating all particles simultaneously. Details and fuller discussion of the algorithm are given in Ref. 16.

B. Ground-state energy

We first calculated the ground-state energy of the system with $N=54$ electrons at a density range of $1\leqslant r_s\leqslant 20$ by both VMC and fixed-node DMC methods. Table II shows the results obtained from the improved trial wave functions in Eq. (4) as well as the Slater-Jastrow wave functions. It can be seen that both VMC and fixed-node calculations with the trial functions including backflow correlation improve significantly the Slater-Jastrow results at all densities considered. However, the three-body correlation is found to have minimal effect for $r_s\leqslant 5$, which corresponds to typical metallic densities.

In Fig. 3 we compare different contributions to the im-

TABLE II. VMC and fixed-node (FN) DMC energies E and the variances of the local energy V obtained with various trial wave functions for $N=54$ (SJ, the Slater-Jastrow function; 3BD, three-body correlation; BF, backflow correlation). The energies are in units of Ry per electron and the variances in units of r_s^4(Ry/electron)^2. ϵ_V is the estimate of the fixed-node error in the backflow fixed-node DMC calculation obtained using Eq. (9).

	$r_s=1.0$	$r_s=5.0$	$r_s=10.0$	$r_s=20.0$
E_{VMC}^{SJ}	1.0669(6)	-0.15558(7)	-0.10745(2)	-0.06333(1)
E_{VMC}^{SJ+3BD}	1.0663(5)	-0.15569(5)	-0.10773(2)	-0.06348(1)
E_{VMC}^{SJ+BF}	1.0617(4)	-0.15729(5)	-0.10829(2)	-0.06365(1)
$E_{VMC}^{SJ+3BD+BF}$	1.0613(4)	-0.15735(5)	-0.10835(2)	-0.06378(2)
E_{FN}^{SJ}	1.0619(4)	-0.15734(3)	-0.10849(2)	-0.06388(1)
$E_{FN}^{SJ+3BD+BF}$	1.0601(2)	-0.15798(4)	-0.10882(2)	-0.06403(1)
V^{SJ}	0.0213(4)	0.0266(3)	0.074(1)	0.189(3)
V^{SJ+3BD}	0.0205(4)	0.0229(4)	0.054(2)	0.144(3)
V^{SJ+BF}	0.0054(3)	0.0069(2)	0.027(1)	0.111(2)
$V^{SJ+3BD+BF}$	0.0053(2)	0.0066(2)	0.026(1)	0.079(2)
ϵ_V	0.0007(6)	-0.00005(8)	0.00002(5)	0.00007(4)

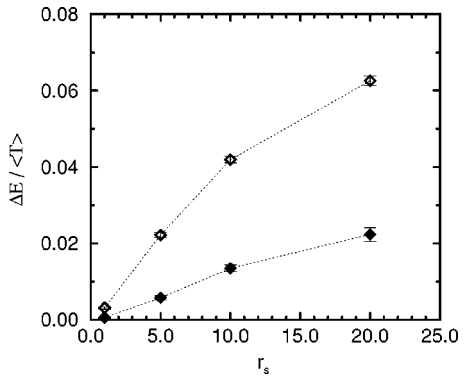

FIG. 4. The energy missing from the Slater-Jastrow wave function ($\diamond$) and from the three-body and backflow wave function ($\blacklozenge$) divided by the kinetic energy as a function of the density parameter r_s. The vertical axis shows $(E_{VMC}-E_{FN}^{3BF})/\langle T\rangle$.

provement in correlation energy beyond the Slater-Jastrow VMC result. The figure shows the changes relative to that given by the backflow fixed-node calculation, which is assumed to be exact in the following discussion. We will examine this assumption at the end of this section. It can be seen that at high densities of $r_s \leqslant 5$, the effect due to the three-body correlation is negligible and the backflow effect is dominant. However, as the density decreases, the three-body effect increases while the backflow effect decreases. We can conclude from the trends of Fig. 3 that at the density where Wigner crystallization occurs, estimated to be $r_s \sim 100$ by Ceperley and Alder,[12] the effect in the energy of the three-body term will be much larger than the backflow term. This is consistent with the expectation that backflow correlation is energetically less important as electrons are localized by strong correlation at low densities. Note, however, that the actual effect of the backflow correlation on the wave function increases at low density, as shown in Fig. 2.

The combined effects of both higher-order correlations in the variational wave function account for 60–80 % of the correlation energy missing in the Slater-Jastrow function. At high densities ($r_s \leqslant 5$), this variational energy is shown to be roughly as good as the Slater-Jastrow fixed-node DMC energy, which captures 70–80 % of the missing correlation energy throughout our density range.

The backflow and three-body effects in the electron gas discussed above are very similar to the situation in two dimensions. See Fig. 4 of Ref. 16. The only notable difference is that at the lowest density considered ($r_s = 20$), the backflow effect is more important than the static three-body correlation in three dimensions while the two correlations have virtually equal importance in two dimensions. This can be understood in terms of the increased importance of correlations in lower dimensions for the same value of r_s; for example, this is reflected in the fact that Wigner crystalization occurs at smaller r_s in two dimensions than in three dimensions.[12,25]

Figure 4 shows the correlation energies missing from the Slater-Jastrow wave function and from the three-body and backflow wave function divided by the kinetic energy. Since the kinetic-energy operator does not commute with the Hamiltonian, the kinetic energy cannot be computed directly with the distribution $\phi_0(R)\Psi_T(R)$ sampled through the diffusion process in Eq. (3). It has been estimated by making an extrapolation using the VMC and the DMC results.[13] It is clear from the figure that the missing correlation energy from both types of trial wave functions becomes a smaller fraction of the kinetic energy at higher densities.

Since our calculation has been done on the system with a finite number of electrons, we extrapolate the energies to the thermodynamic limit to compare with other calculations. We follow the extrapolation scheme based upon the Fermi-liquid theory,[26,25] which assumes that the energy per particle for a finite system with the periodic boundary conditions is related to the bulk energy by

$$E_N = E_\infty + b_1(r_s)\Delta T_N + b_2(r_s)\frac{1}{N}. \tag{8}$$

Here, E_N (E_∞) is the total energy per electron of the finite (infinite) system and ΔT_N is the free-particle kinetic-energy differences between two systems. We determine the parameters E_∞, b_1, and b_2 by a least-squares fit to VMC calculations with Slater-Jastrow (SJ) trial functions at different values of $N = 54,66,114,162,246$. In Table III are shown the energies, fitted parameters, and the χ^2 value of the fit. The reasonable values of χ^2 show that the Fermi-liquid theory completely explains the size dependence of the energy to statistical accuracy of the VMC energies over this range of particle numbers. To extract the extrapolated three-body and backflow DMC energy for the infinite system, $E_\infty^{3BF\text{-}DMC}$, we did the DMC runs only at $N = 54$ whose results are shown in Table II and then use the parameters determined from VMC to get $E_\infty^{3BF\text{-}DMC}$. It is assumed that the size dependences for the VMC (SJ) and the DMC (3BF) results are the same. This assumption needs to be tested in future calculations. The same procedure was successfully applied to assess the finite-size effects in our previous QMC calculation for the two-dimensional electrons[16].

One can see in Table III that our extrapolated backflow fixed-node energies are lower, even if the differences are small, than Ceperley and Alder's released-node results as well as Ortiz and Ballone's Slater-Jastrow fixed-node results. The systematic differences between these independent calculations are found to be mostly due to the difference in the way of correcting for the finite-size errors. As a matter of fact, our backflow fixed-node energies for 54 electrons given in Table II are virtually identical to the corresponding released-node results of Ceperley and Alder within statistical errors. Considering that a fixed-node energy is an upper bound to the true ground-state energy, this validates our assertion that our backflow fixed-node results are accurate. Our present results show that the calculations of Ceperley and Alder only got approximately half of the Slater-Jastrow fixed-node error with their released-node procedure due to computer limitations at that time.

Since the fixed-node results depend only on the nodal structures of the trial functions used, one can speculate that the nodal locations of the backflow wave function are fairly close to those of the exact ground state. Without more investigation, we cannot quantify this statement, because there is not a simple relationship between nodal locations and fixed-node energy. The accuracy of the backflow nodes was also

TABLE III. Size dependence in the Slater-Jastrow VMC method of normal electron liquid at $1 \leqslant r_s \leqslant 20$ and χ^2-fit parameters. Also shown are the extrapolated DMC energies at an infinite system ($E_\infty^{SJ\text{-}DMC}$ and $E_\infty^{3BF\text{-}DMC}$), Ceperley and Alder's released-node result (CA*), and Ortiz and Ballone's Slater-Jastrow fixed-node result (OB**).

		$r_s=1.0$	$r_s=5.0$	$r_s=10.0$	$r_s=20.0$
E_{VMC}^{SJ}	$N=54$	1.0669(6)	-0.15558(7)	-0.10745(2)	-0.06333(1)
	$N=66$	1.1496(5)	-0.15166(4)	-0.10637(2)	-0.06303(1)
	$N=114$	1.2079(5)	-0.14867(3)	-0.10552(2)	-0.06278(1)
	$N=162$	1.1162(4)	-0.15238(3)	-0.10642(1)	-0.06270(1)
	$N=246$	1.1938(3)	-0.14886(3)	-0.10548(1)	-0.06275(1)
$E_\infty^{SJ\text{-}VMC}$		1.1795(4)	-0.14914(3)	-0.10549(2)	-0.06273(1)
$b_1(r_s)$		1.096(6)	1.18(1)	1.21(2)	1.22(3)
$b_2(r_s)$		-1.16(5)	-0.134(4)	-0.051(2)	-0.0181(7)
χ^2		1.20	1.29	2.22	2.26
$E_\infty^{SJ\text{-}DMC}$		1.1744(4)	-0.15094(4)	-0.10654(2)	-0.06329(1)
$E_\infty^{3BF\text{-}DMC}$		1.1726(2)	-0.15158(5)	-0.10687(2)	-0.06344(1)
CA*		1.174(1)	-0.1512(1)	-0.10675(5)	-0.06329(3)
OB**		1.181(1)	-0.1514(3)		

shown in our previous released-node (transient-estimate) calculation for the two-dimensional electron gas.[27]

Although comparison with well-converged exact results is the best method of assessing the accuracy of a fixed-node result for the energy, in the remainder of this section we develop another estimate that requires only the VMC energy and the variance of the local energy. This relies on the observation that both the error in the variational energy E_{VMC} and the variance V are quadratic in the difference between a trial function and the true ground state. Thus, as a trial function is improved in going from a two-body level (Slater-Jastrow) to a higher-order level (backflow and three-body), one can estimate the exact energy by the improvements of the variational energy relative to the variance.

The variances of the local energy for the various trial wave functions are given in Table II and plotted in Fig. 5 at $r_s=10$. As can be seen, the variance decreases roughly proportional to the drop in energy for the four trial functions considered. The dotted line in Fig. 5 represents a linear fit and the triangle our best (backflow) fixed-node energy. There is no fundamental reason why the energy and variance for general trial functions would have a linear relationship. However, in practice this relation is often observed.[16] The observed linear relationship both validates our optimization procedure and provides an independent estimate of the exact energy.

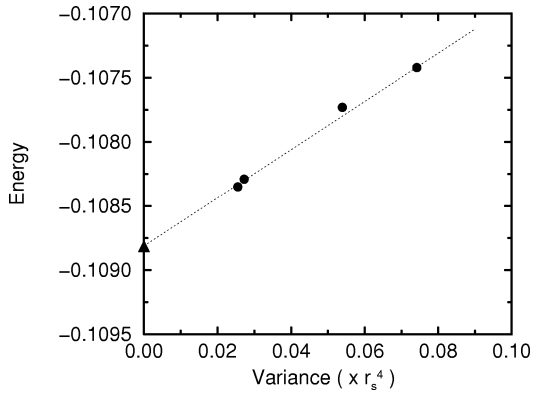

FIG. 5. Variational energy versus the variance of local energy at $r_s=10$. Each point ● represents one variational calculation: from higher to lower energies, the Slater-Jastrow, three-body, backflow, and (backflow + three-body) results. The filled triangle represents our backflow fixed-node result and the dotted line shows a linear fit through ● points. The statistical errors of the data are smaller than the sizes of the symbols.

The exact ground-state energy E_0 is estimated using the following assumption:

$$\frac{V^{(k)}}{E_{VMC}^{(k)}-E_0}=\text{const.} \tag{9}$$

We extrapolated using only the results from the best (backflow + three-body) and worst (Slater-Jastrow) trial functions to minimize the extrapolation error. Shown in Table II, ϵ_V is our estimate of the error of the computed backflow fixed-node energy, which is an upper bound to the true ground-state energy. (There is also the Temple lower bound[28] to the ground-state energy, which involves the energy and the variance. However, it is not useful for many-body systems.) Because our procedure is not rigorous, there is no guarantee that the estimated energy will lie below our computed best fixed-node result. In fact at $r_s=5$ the estimate lies above it. It can be seen in Table II that the estimated fixed-node error is much smaller at all densities than the energy improvements due to the nodal change from the Slater-Jastrow function to the backflow wave function. This is another evidence that our fixed-node DMC calculations using the backflow trial functions give very accurate results for the ground-state energy.

IV. CONCLUSION

We have studied the correlation energy of the interacting three-dimensional electron gas, using VMC and fixed-node DMC calculations including the three-body and the backflow correlation. The additional correlation energy due to backflow is dominant over the three-body effect in the high-density regime but the relative importance of the former decreases as the density is reduced. This is the same trend as was found for the two-dimensional electron gas[16] except that the importance of backflow is more significant in higher dimensions, especially at low densities. This is due to the fact that in two dimensions the effects of interactions are larger than in three dimensions at a given r_s and other effects tend to dominate more over the effects of backflow.

The variational wave function with backflow and three-body correlations is a large improvement over the Slater-Jastrow function. We find that these higher-order correlations account for 60–80 % of the remaining correlation energy beyond the Slater-Jastrow variational results. Since backflow changes the nodes, the fixed-node DMC results are also significantly improved. The fixed-node method based upon the Slater-Jastrow nodes is found to capture no more than 80% of the remaining correlation energy.

After making a careful finite-size analysis, we have compared our backflow fixed-node energies with Ceperley and Alder's released-node results. These two independent calculations using different methods are found to give nearly identical results within statistical and systematic errors. From a linear extrapolation to zero variance of the local energy, we find further evidence that our backflow fixed-node results are very close to the true ground-state energy.

For future work, we conclude that one should be able to use much improved wave functions, better released-node methods,[29] with more size-dependence studies and full utilization of current computer hardware to achieve an order of magnitude more accurate results for the energy of the electron gas than was done nearly two decades ago.

ACKNOWLEDGMENTS

This work has been supported by the Korea Science and Engineering Foundation under Grant No. 96-0207-045-2, through its SRC program, and by the National Science Foundation under Grant No. DMR 94-224-96.

[1] D. Pines, *Elementary Excitations in Solids* (Addison-Wesley, New York, 1963).
[2] W. Kohn and L. J. Sham, Phys. Rev. **140**, A1133 (1965).
[3] R. G. Parr and W. Yang, *Density-Functional Theory of Atoms and Molecules* (Oxford University Press, New York, 1989).
[4] F. Bloch, Z. Phys. **57**, 545 (1929).
[5] E. Wigner, Phys. Rev. **46**, 1002 (1934); Trans. Faraday Soc. **34**, 678 (1938).
[6] A. W. Overhauser, Phys. Rev. Lett. **3**, 414 (1959); **4**, 462 (1960); Phys. Rev. **128**, 1437 (1962).
[7] K. Moulopoulos and N. W. Ashcroft, Phys. Rev. Lett. **69**, 2555 (1992).
[8] G. D. Mahan, *Many-Particle Physics* (Plenum, New York, 1991).
[9] M. Gell-Mann and K. A. Brueckner, Phys. Rev. **106**, 364 (1957).
[10] K. S. Singwi, M. P. Tosi, R. H. Land, and A. Sjölander, Phys. Rev. **176**, 589 (1968).
[11] D. M. Ceperley, Phys. Rev. B **18**, 3126 (1978).
[12] D. M. Ceperley and B. J. Alder, Phys. Rev. Lett. **45**, 566 (1980).
[13] K. Schmidt and M. H. Kalos, in *Applications of the Monte Carlo Method in Statistical Physics*, edited by K. Binder (Springer-Verlag, Berlin, 1984).
[14] J. B. Anderson, J. Chem. Phys. **63**, 1499 (1975); **65**, 4121 (1976).
[15] P. J. Reynolds, D. M. Ceperley, B. J. Alder, and J. W. A. Lester, J. Chem. Phys. **77**, 5593 (1982).
[16] Y. Kwon, D. M. Ceperley, and R. M. Martin, Phys. Rev. B **48**, 12 037 (1993).
[17] D. M. Ceperley, in *Recent Progress in Many Body Theories*, edited by J. Zabolitzky, Lecture Notes in Physics Vol. 142 (Springer-Verlag, Berlin, 1981).
[18] G. Ortiz and P. Ballone, Europhys. Lett. **23**, 7 (1993); Phys. Rev. B **50**, 1391 (1994).
[19] S. Moroni, S. Fantoni, and G. Senatore, Phys. Rev. B **52**, 13 547 (1995).
[20] D. M. Ceperley, J. Stat. Phys. **63**, 1237 (1991).
[21] T. Gaskell, Proc. Phys. Soc. London **77**, 1182 (1961).
[22] R. P. Feynman and M. Cohen, Phys. Rev. **102**, 1189 (1956).
[23] P. Ewald, Ann. Phys. (Leipzig) **64**, 253 (1921).
[24] C. J. Umrigar, K. G. Wilson, and J. W. Wilkins, Phys. Rev. Lett. **60**, 1719 (1988).
[25] B. Tanatar and D. M. Ceperley, Phys. Rev. B **39**, 5005 (1989).
[26] D. M. Ceperley and B. J. Alder, Phys. Rev. B **36**, 2092 (1987).
[27] Y. Kwon, D. M. Ceperley, and R. M. Martin, Phys. Rev. B **53**, 7376 (1996).
[28] G. Temple, Proc. R. Soc. London, Ser. A **119**, 22 (1928).
[29] M. Caffarel and D. M. Ceperley, J. Chem. Phys. **97**, 8415 (1992).